ELECTRON TRANSPORT IN XANTHINE OXIDASE

A MODEL FOR OTHER BIOLOGICAL ELECTRON TRANSPORT CHAINS

ALAN VAN HEUVELEN

From the Physics Department, New Mexico State University, Las Cruces, New Mexico 88003

ABSTRACT Part of the catalytic function of xanthine oxidase (XO) involves the transfer of two electrons from a substrate to a molybdenum ion on the enzyme followed by equilibration of these electrons among other electron resting sites on the enzyme. The electrons are removed from the enzyme at a flavin by oxygen to form hydrogen peroxide. This paper considers mechanisms which allow the electrons to equilibrate between the different resting sites on the enzyme. The mechanisms are chosen to be consistent with known properties of the enzyme (relative reduction potentials, electron transfer rates, and the estimated separation of these resting sites). Tunneling appears to be a good candidate to account for most of the electron transport. It is shown that the XO electron transport system is similar in many respects to sections of mitochondrial electron transport chains and can serve as a nice model for parts of these more complicated biological electron transport systems.

INTRODUCTION

Xanthine oxidase (XO) is a complicated enzyme whose function is pictured schematically in Fig. 1. The enzyme has two independent catalytic centers. Each center has a molybdenum ion, two distinct iron-sulfur centers, and a flavin group (1). A substrate such as xanthine deposits two electrons (or a hydide ion) at the molybdenum. The electrons equilibrate rapidly among the different groups on the enzyme and are picked up by oxygen at the flavin. We will be concerned here only with mechanisms which can account for electron transport through the protein and not with enzyme reduction and oxidation processes. We will consider the experimental and theoretical techniques used to calculate the relative reduction potentials of the different electron resting sites in XO, the time required for electrons to move between these different sites, possible electron transport mechanisms consistent with these times and potentials, and, finally, a comparison of the XO electron transport system with electron transport chains found in mitochondria.

RELATIVE REDUCTION POTENTIALS (EXPERIMENTAL)

The four electron resting sites per active center can accept electrons from three different substrates, i.e. up to six electrons (two electrons each at the molybdenum and flavin sites and one electron at each of the two Fe/S sites). The valence states of resting sites

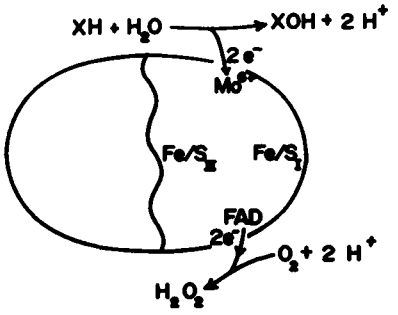

FIGURE 1 A schematic representation of the catalytic function of xanthine oxidase. A substrate such as xanthine (XH) is changed to uric acid (XOH) during catalysis.

with one extra electron (Mo^{5+}, $FADH^{\cdot}$, $Fe/S_I^{\cdot}$, and $Fe/S_{II}^{\cdot}$) are paramagnetic and the kinetics of their reduction and oxidation have been studied extensively by rapid freeze, electron paramagnetic resonance (EPR) experiments (2-4) and more recently by a rapid freeze, slow warm process (5).

Olson et al. (6) anaerobically titrated XO with xanthine and used the populations of different resting sites as measured by EPR and visible spectroscopy to determine the relative reduction potentials of the different sites. We have made similar calculations using results of rapid freeze, slow warm experiments. The preparations and techniques used are as described previously (5), with one exception which will be described shortly. In these experiments XO and xanthine are mixed and their reaction is quenched in a rapid freeze apparatus after a predetermined delay time. If for example, the reaction is quenched 10 ms after mixing, most active sites have received either two electrons or no electrons (the half time for one substrate turnover is about 20 ms [6]). The diffusion and binding constants are such that there is a substrate at each active site. When this frozen solution is warmed at $-50°$ C for 30 min, additional reduction of XO by these bound substrates occurs such that every active site has received two electrons (5).

There is normally considerable oxygen in the isopentane quenching solution of the rapid freeze apparatus (5, 7). To remove the oxygen, dry nitrogen gas was cooled in a heat exchange coil immersed in liquid nitrogen and then bubbled through the $-140°$ C isopentane solution used for quenching the reaction. 10 ms quenching in this anaerobic isopentane followed by warming at $-50°$ C results in two-electron reduced enzyme. If oxygen is left in the $-140°$ C isopentane quenching solution, then as the sample is warmed one electron is removed from each active center in the fast reoxidation process discussed by Olson et al. (8) (and also in ref. 5 relative to the slow warm process). Thus, it is also possible to get enzymes which have one electron per active site. Similarly if one allows long delays after mixing (200 ms or more) before quenching, then each enzyme gets six electrons. If the quenching occurs in isopentane with oxygen, then roughly 50% of these active centers lose two electrons (i.e., retain four electrons) to oxygen during the 5 ms quenching time (5). EPR was used to measure the electron distributions in these three samples (with one. two, and 50% four-50% six electrons).

These distributions are reported in Table I. The amount of $FADH_2$ plus Mo^{4+} species present was that required to bring the total number of electrons to 1, 2, or (4 + 6)/2 = 5.

RELATIVE REDUCTION POTENTIALS (CALCULATIONS)

It is assumed that each oxidized electron resting site (FAD, Mo^{6+}, Fe/S_I, and Fe/S_{II}) can accept either one or two electrons. For one-electron reduced resting sites the electron goes into one of two degenerate energy states (corresponding to the two-electron spin states, ↑ or ↓). These one-electron energy states are labeled: $m\uparrow$ or $m\downarrow$ (Mo^{5+}); $f\uparrow$ or $f\downarrow$ ($FADH^{\cdot}$); $I\uparrow$ or $I\downarrow$ ($Fe/S_I^{\cdot}$); and $II\uparrow$ or $II\downarrow$ ($Fe/S_{II}^{\cdot}$). The doubly reduced resting sites are labeled: $F\uparrow$ -$F\downarrow$ ($FADH_2$); $M\uparrow$ -$M\downarrow$ (Mo^{4+}); $I'\uparrow$ -$I'\downarrow$ ($Fe/S_I^{\cdot\cdot}$); and $II'\uparrow$ -$II'\downarrow$ ($Fe/S_{II}^{\cdot\cdot}$). The one-electron energies of these paired electrons are different from the one-electron energies of a singly reduced site (e.g. $E_f \neq E_F$). Since one never observes doubly reduced Fe/S centers in XO, the energies $2E_{I'}$ and $2E_{II'}$ must be very high.

Each active center can theoretically accept up to eight electrons (although as mentioned, the Fe/S centers take only one). If we let n equal the actual number of electrons per active center, then the number of possible states for these n electrons is

$$N = 8!/(8\text{-}n)!n!.$$

The values of N for different n are $(n,N) = (0,1); (1,8); (2,28); (3,56); (4,70); (5,56); (6,28); (7,8); (8,1)$. These numbers differ considerably from those of Olson et al. (6) who neglected the double degeneracy of singly reduced resting sites. The relative reduction potentials calculated from our statistics differ some from those of Olson et al., but not to the extent that they have a significant affect on our later discussions about possible electron transport mechanisms.

The probability of observing a particular ionization state of a resting site when n electrons are on the enzyme active center is given by Eq. 1 below. The subscript j labels the different ionization states of individual resting sites (i.e., $j = m, f$, I, II, M, F, I', or II').

$$P_{nj} = \sum_{\text{all states with species } j} \exp[-(\ldots + E_j + \ldots)/kT]/Z_n. \qquad (1)$$

The energy term in the exponent $(\ldots + E_j + \ldots)$ is the sum of one-electron energies for a state in which the jth species appears (there should be n one-electron energies). k is Boltzmann's constant and T is the temperature in degrees Kelvin. Z_n is the partition function for an active center with n electrons and is

$$Z_n = \sum_{\substack{\text{all states} \\ \text{with } n \text{ electrons} \\ \text{per active center}}} \exp[-(\ldots + E_j + \ldots)/kT]. \qquad (2)$$

As an example of these calculations we consider the two-electron reduced active center, i.e. for $n = 2$. There are 28 possible states for distributing these two electrons.

TABLE I

OCCUPATIONS OF DIFFERENT ELECTRON RESTING SITES

pH	No. of electrons per active site	Observed and (calculated*) electron occupation probabilities				
		Mo^{5+}	FADH$^{\cdot}$	$Fe/S_I^{\cdot}$	$Fe/S_{II}^{\cdot}$	$(Mo^{4+} + FADH_2)$‡
6.3	1	0.06(0.05)	0.02(0.04)	0.31(0.32)	0.61(0.59)	(0.00)
6.3	2	0.11(0.09)	0.03(0.04)	0.50(0.37)	0.65(0.41)	0.36(0.04 + 0.49)
6.3	(4 + 6)/2	0.14(0.15)	0.04(0.01)	0.72(0.86)	0.86(0.92)	1.62(0.55 + 0.98)
10.1	1	0.11(0.10)	0.03(0.04)	0.24(0.27)	0.61(0.59)	(0.00)
10.1	2	0.14(0.15)	0.04(0.07)	0.40(0.33)	0.55(0.41)	0.44(0.03 + 0.49)
10.1	(4 + 6)/2	0.12(0.09)	0.02(0.01)	0.90(0.90)	0.90(0.92)	1.53(0.58 + 0.96)

*Calculations based on energies in Table II.

‡The actual number of electrons in Mo^{4+} + $FADH_2$ species is twice the numbers given here.

Letting $u = 1/kT$ we have

$$Z_2 = [e^{-u2E_M} + e^{-u2E_F} + e^{-u2E_{I'}} + e^{-u2E_{II'}} + 4e^{-u(E_m + E_f)} + 4e^{-u(E_m + E_I)} + 4e^{-u(E_m + E_{II})} + 4e^{-u(E_f + E_I)} + 4e^{-u(E_f + E_{II})} + 4e^{-u(E_I + E_{II})}].$$

The probabilities for observing the different resting site ionization states are:

$$Mo^{4+}: \quad P_{2M} = e^{-u2E_M}/Z_2$$

$$FADH_2: \quad P_{2F} = e^{-u2E_F}/Z_2$$

$$Mo^{5+}: \quad P_{2m} = [4e^{-u(E_m + E_f)} + 4e^{-u(E_m + E_I)} + 4e^{-u(E_m + E_{II})}]/Z_2$$

$$Fe/S_I^{\cdot}: \quad P_{2I} = [4e^{-u(E_m + E_I)} + 4e^{-u(E_f + E_I)} + 4e^{-u(E_I + E_{II})}]/Z_2,$$

etc.

Comparing the above probabilities for the two-electron distributions and similar probabilities for the one- and the 50% four-50% six-electron distributions with the observed populations given in Table I, we are able to calculate the one-electron energies. These results are given in Table II. In order to calculate E_M and E_F we have assumed that $e^{-2E_M}/e^{-2E_F} \simeq 0.1$. This is based on the observed populations of the Mo^{4+} ionization state relative to the $FADH_2$ state as given in Fig. 3 of ref. 6.

It is possible to check the results of Table II against the titration experiments of Olson et al. (Fig. 3 in ref. 6). To do this one must include the possibility that electrons are distributed unevenly among the different active centers; e.g., after giving an average of two electrons per active site to the enzymes, these electrons can rearrange themselves so that some sites have three electrons while others have one, etc. The fraction of active sites choosing zero, one, two, three, ..., or eight electrons depends on the relative energies and on the number of ways each situation can be formed. One procedure for performing these calculations is developed in the Appendix. We have used this pro-

TABLE II

RELATIVE REDUCTION POTENTIALS OF ELECTRON ACCEPTOR GROUPS IN XO

	Relative one-electron energies		
	pH 6.3	pH 10.1	pH 8.5 (ref. 6)
	mV	*mV*	*mV*
$FADH^{\cdot}$ (E_f)	70	65	60
Mo^{5+} (E_m)	60	45	60
$Fe/S_I^{\cdot}$ (E_I)	15	20	24
Mo^{4+} (E_M)	15	10	45
$Fe/S_{II}^{\cdot}$ (E_{II})	0	0	0
$FADH_2$ (E_F)	−15	−15	0
	Relative reduction potentials		
	mV	*mV*	*mV*
$Fe/S_{II}^{\cdot} + FAD + H^+ \rightleftarrows FADH^{\cdot} + Fe/S_{II}$	−70	−65	−60
$Fe/S_{II}^{\cdot} + Mo^{6+} \rightleftarrows Mo^{5+} + Fe/S_{II}$	−60	−45	−60
$Fe/S_I^{\cdot} + Fe/S_I \rightleftarrows Fe/S_I^{\cdot} + Fe/S_{II}$	−15	−20	−24
$Fe/S_{II}^{\cdot} + Fe/S_{II} \rightleftarrows Fe/S_{II}^{\cdot} + Fe/S_{II}$	0	0	0
$Fe/S_{II}^{\cdot} + Mo^{5+} \rightleftarrows Mo^{4+} + Fe/S_{II}$	30	25	−31
$Fe/S_{II}^{\cdot} + FADH^{\cdot} + H^+ \rightleftarrows FADH_2 + Fe/S_{II}$	100	95	60

cedure for several values of $\bar{n}$ ($\bar{n}$ is defined as the average number of electrons per active site) along with our values of E_j, and find that these calculated $P_{\bar{n}j}$ values agree fairly well with the numbers shown in Fig. 3 of ref. 6.

There are three important results to note from Table II. First we see that the relative reduction potentials of the different centers are all within 160 mV of each other. Using the energies in Table II, one can devise schemes for transferring two electrons from Mo^{4+} to $FADH_2$ in one-electron "hops" which involve no more than a 100 mV change in potential per hop (most hops involve somewhat less energy change).

Secondly, we see that the relative reduction potentials depend on pH. This result is obvious to anyone who has taken EPR spectra of XO at different values of pH. We mention it here only to emphasize a possible control mechanism for electron transport. One can envision a process in which changes in proton concentrations or concentrations of other chemicals which interact with electron transport chain resting sites alter the relative reduction potentials, thus slowing, stopping, or perhaps even reversing the direction of electron transport.

Thirdly, the XO electron transport chain has been arranged such that the point of departure of electrons from the chain (the $FADH_2$ species) is an energetically preferred state and electrons can find their way from the Mo^{4+} to $FADH_2$ by merely looking for states with lower energy.

HOPPING TIME

We estimate that the time required for electron transport between different resting sites, t_{et}, must be faster than 5×10^{-3} s. This is based on several observations: (*a*) pH

jump experiments reported by Edmundson et al. (4) indicate that electrons reequilibrate among the different resting sites when the pH is changed in times less than 5×10^{-3} s. (*b*) The recent successful description of the whole catalytic process of XO by Olson et al. (6, 8) has assumed rapid equilibration times. (*c*) Our own rapid freeze-slow warm experiments indicate that electrons redistribute among the various resting sites at least as fast as the rate of the reoxidation of the enzyme (5), the half time of which is about 5×10^{-3} s at room temperature (8).

It is not possible to establish a lower time limit to the electron hopping time. An estimate can be made based on the fact that the EPR spectra of the different paramagnetic species in XO are similar to spectra one finds of similar isolated species (with the exception of the $Fe/S_{II}^{\bullet}$ spectra which seems somewhat unique); e.g. the $FADH^{\bullet}$ EPR spectra is similar to that of other isolated flavin complexes. If the electron was jumping between centers faster than the spin-lattice relaxation time of the $FADH^{\bullet}$ paramagnetic species, then we would expect to see some unusual compromise EPR spectra which reflected the environment of more than one paramagnetic center (ref. 9 and references therein). This is not seen.

Spin-lattice relaxation times depend on temperature and are typically 10^{-8}–10^{-10} s at room temperature, although there is great variation. In choosing possible mechanisms for electron transport we will be eliminating mechanisms because they are too slow (i.e. slower than the 5×10^{-3} s limit), and not too fast. The lower limit (10^{-8}–10^{-10} s) is approximate but does not really affect our further discussions. We will then say that the electron hopping takes place between the limits in Eq. 3 below.

$$10^{-10}\,\text{s} < t_{et} < 5 \times 10^{-3}\,\text{s}. \tag{3}$$

ELECTRON TRANSPORT MECHANISMS

The potential energy surfaces between resting sites and even in the vicinity of particular resting sites are not known for complicated systems such as are found in proteins. Thus we will consider electron transport mechanisms based on simple model potentials in order primarily to see which mechanisms give transport rates consistent with rates discussed in the previous section. In particular we will consider each resting site to be a potential well for an electron, the different potential wells being separated by parabolic shaped energy barriers of different heights and widths (see Fig. 2). The barrier shape can have some effect on the electron tunneling rates (a factor of 10 or more), and since these shapes are not known our numbers are at best order of magnitude. We have chosen a parabolic shape because it seems compatible with the delocalized nature of electron resting states found in proteins (10).

Semiconduction Over the Top of a Barrier

The rate c for an electron to move between two neighboring wells by going over the top of a barrier between them (Fig. 2*a*) is given approximately by

$$c \cong [(1/D)\,(kT/2\pi m)^{1/2}]\,e^{-(V_o - E_o)/kT}. \tag{4}$$

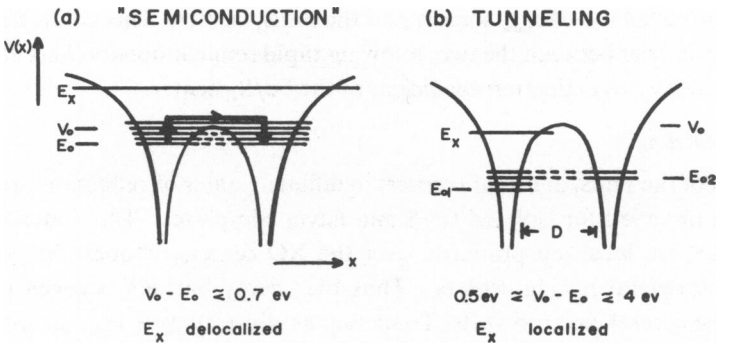

FIGURE 2 A schematic representation of possible electron transport mechanisms: (*a*) semiconduction, and (*b*) tunneling. The wells are electron resting sites and are separated by potential energy barriers. E_x represents an electronically excited state.

The bracket term is the reciprocal of the time required to cross a barrier of width D (11). c depends primarily on the probability for an electron being thermally excited over a barrier of height $V_o - E_o$. From Table III we see that the rates are too slow for barriers that are over 0.6–0.7 eV high. For barriers lower than this, going over the top is usually faster than tunneling through the barrier (12).

For a barrier 0.7 eV or less in height, one should observe unusual electron absorption spectra since the excited state E_x (several electron volts above the ground state) will be delocalized over more than one electron resting site (Fig. 2*a*). The band shape and position should be different than that observed for isolated complexes and its intensity should be reduced since the ground state will overlap somewhat less with such a delocalized excited state. This seems to be the situation with the Fe/S_{II} center in XO whose absorption band at 550 nm is about one-fourth the intensity of that usually observed for other Fe/S centers in proteins (6). Recent measurements using ENDOR and ELDOR (9, 13; L. Armstrong and R. H. Sands, personal communication) indicate that there may be a rapid cross relaxation between a particular form of

TABLE III
RATES c FOR CROSSING OVER DIFFERENT SIZE BARRIERS BETWEEN POTENTIAL WELLS (SEMICONDUCTION)

$V_o - E_o$	D	c	$t_{et} = 1/c$
eV	*Å*	s^{-1}	*s*
2	10	4.9×10^{-22}	2×10^{22}
1	10	1.1×10^{-4}	9×10^{3}
0.7	10	1.9×10^{1}	5×10^{-2}
0.6	10	1.0×10^{3}	1×10^{-3}
0.5	10	5.5×10^{4}	2×10^{-5}
0.5	30	1.8×10^{4}	6×10^{-5}
0.3	10	1.6×10^{8}	6×10^{-9}
0.3	30	5.5×10^{7}	2×10^{-8}

the Mo^{5+} ion called the Mo_{slow} species and the Fe/S_{II} center. This could be a result of a low energy barrier between the two, allowing rapid semiconduction and also explaining the unusually low extinction coefficient of the Fe/S_{II} center.

Tunneling

The spectra of the Fe/S_I and FAD centers in different states of reduction are very similar to those observed for isolated Fe/S and flavin complexes. This indicates that the excited states are localized primarily over the XO centers in question and not distributed over several resting centers. Thus the energy barriers between neighboring sites must be several electron volts. Tunneling as illustrated in Fig. 2*b* could explain electron conduction involving these centers. The tunneling rate

$$c = \nu \frac{\exp\{-(\pi^2/h)D[2m(V_o - E_o)]^{1/2}\}}{1 - (\pi^2 kTD/h)[2m/(V_o - E_o)]^{1/2}} [\exp(-|E_{o2} - E_{o1}|/kT)] \qquad (5)$$

depends on the vibrational frequency ν inside one well (assumed to be 10^{15} s^{-1} [12]), the probability of tunneling through a parabolic barrier $V_o - E_o$ high and D wide, and finally on any vibrational activation energy $(E_{o2} - E_{o1})$ needed to align the ground state energies on each side of the well so that the electron can conserve energy while tunneling. We have seen earlier that the relative reduction potentials for one electron hops are roughly 50 mV ($\sim E_{o2} - E_{o1}$).

Table IV indicates different barrier heights, widths, and ground state activations ($|E_{o2} - E_{o1}|$) for which tunneling can account for electron transport in XO. Tunneling rates in Table IV fit our requirements for wells that are anywhere from 1 to 4 eV high and up 30 Å wide. Thus tunneling certainly seems like a good candidate for much of the electron transport in XO.

MITOCHONDRIAL ELECTRON TRANSPORT

Bennett (14) has given a nice representation of the mitochondrial electron transport system including the respiratory redox centers. The electron transport system consists

TABLE IV
BARRIER WIDTHS AND HEIGHTS FOR WHICH THE TUNNELING RATE c IS $0.2 \times 10^3\ s^{-1} \leq c \leq 10^8\ s^{-1}$

D	$V_o - E_o$ limits	$\lvert E_{o2} - E_{o1} \rvert$
Å	*eV*	*mV*
30	$V_o - E_o < 1.4$	0
20	$1 < V_o - E_o < 3$	0
15	$1.9 < V_o - E_o < 4$	0
10	$3.3 < V_o - E_o <$	0
30	$V_o - E_o < 1.2$	75
20	$0.7 < V_o - E_o < 2.5$	75
15	$1.1 < V_o - E_o < 3.5$	75
10	$2.8 < V_o - E_o$	75

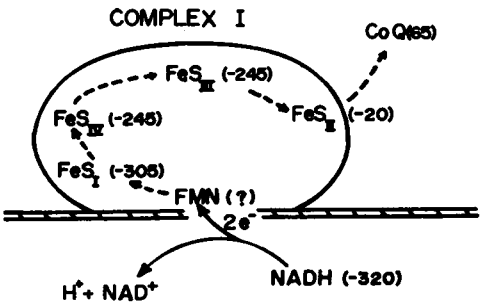

FIGURE 3 A schematic representation of complex I of the mitochondrial electron transport chain. The numbers in parantheses are electron reduction potentials.

of four complexes, each of which has at least four electron resting sites (flavins, iron-sulfur centers, cytochromes and/or copper ion centers). Pairs of electrons enter either complex I or complex II and come out at complex IV. Electrons are transmitted between complexes by ubiquionones or cytochrome *C* in some not yet understood process.

We will concern ourselves here only with electron transport through sections of a particular complex in which there is no chemical process coupled to phosphorylation. In particular we will consider complex I, shown schematically in Fig. 3. An electron pair is given the FMN in complex I by NADH. Electrons leave complex I at an iron sulfur center $(FeS)_{II}$ and pass to a coenzyme Q_{10} molecule (a ubiquinone). The reduction potentials (15 and references therein) of the different resting sites in complex I are shown in Fig. 3 (in parenthesis) along with the presumed electron path. The 225 mV drop in potential between the $(FeS)_{III}$ and $(FeS)_{II}$ centers is supposedly coupled to a phosphorylation reaction. However, for the other resting sites in complex I the reduction potentials are within 65 mV of each other (similar to the numbers measured in xanthine oxidase). Other similarities of the two electron transport systems are compared in Table V; e.g., the maximum possible average separation of electron resting

TABLE V
COMPARISON OF XANTHINE OXIDASE AND MITOCHONDRIAL ELECTRON TRANSPORT CHAIN

Molecular weight	380,000	800,000
No. of electron resting sites	8	$\simeq 20$
Dimensions	$2R \simeq 100$ Å	$\sim 230 \times 60 \times 60$ Å^3
Largest possible average separation of electron resting sites	50 Å	35 Å
Potential drop across metal ion centers (no phosphorylation)	30–100 mV	40–75 mV
Protons pumped per electron pair	2 H^+	6 H^+

sites in the two systems (based on the size of the protein and the number of resting sites) are similar (undoubtedly less than the numbers in Table IV).

In conclusion, using the XO electron transport system as a model for electron transport in mitochondria, we would say that electrons in sections of the mitochondrial electron transport chain not involved in phosphorylation can equilibrate between different centers mainly by tunneling in times less than milliseconds. The relative reduction potentials are very similar in these regions (to allow rapid transfer) but favor electron sites near the site involved in phosphorylation. Such a region exists in complex I at the $(FeS)_{III}$ site which is a favorable location in terms of energy for an electron. The $(FeS)_{III}$ to $(FeS)_{II}$ electron jump (225 mV) must result in an energy transfer used for the phosphorylation reaction, and is a rate limiting step in electron transport just as the enzyme reduction step is rate limiting in xanthine oxidase.

APPENDIX

In what follows we will develop a technique for calculating one-electron energies E_j for the different ionization states of electron resting sites (labeled j). In these calculations one varies the E_j until the theoretical and experimentally observed probabilities $P_{\bar{n}j}$ match. The $P_{\bar{n}j}$ give the probability for observing a species j when there are on the average $\bar{n}$ electrons per active center. It is assumed that active centers can exchange electrons and that for a particular $\bar{n}$, centers may have anywhere from $n = 0$ to 8 electrons. The following notation is used.

N_b The total number of active centers (for XO N_b is two times the number of enzymes in the sample).

N_e The total number of electrons (varies from 0 N_b to 8 N_b in principal but only to 6 N_b in experiment).

n Number of electrons in a particular active center and can be 0, 1, 2, . . . , 8.

N_n Number of active centers with n electrons.

F_n Helmholtz free energy of a single active center with n electrons and is given by

$$F_n = -kT \ln Z_n. \tag{6}$$

Z_n The partition function for a single active center with n electrons; Z_n is defined by Eq. 2 in the text.

F Helmholtz free energy of the N_e electrons and is given by

$$F = \sum_{n=0}^{8} N_n F_n - TS. \tag{7}$$

T The temperature in °K; S is the entropy and is given by

$$S = k \ln G. \tag{8}$$

G The number of unique ways in which N_e numbered electrons can be distributed between the N_b active centers such that a particular distribution set $\{N_0, N_1, \ldots, N_8\} = \{N_n\}$ is achieved; G is given by

$$G = N_b! \prod_{n=0}^{8} N_n!$$

Because G varies for different sets $\{N_n\}$, we find that F depends not only on the energy (the $\Sigma N_n F_n$ term of Eq. 7) but also on the number of ways to statistically distribute the electrons between the active centers (the TS part of equation 7).

At thermal equilibrium the free energy F should be minimized subject to the following two conditions:

$$\sum_{n=0}^{8} N_n - N_b = 0 \equiv g_1(N_0, \ldots, N_8), \tag{10}$$

$$\sum_{n=0}^{8} n N_n - N_e = \sum_{n=0}^{8} n N_n - \bar{n} \sum_{n=0}^{8} N_n = 0 = g_2(N_0, \ldots, N_8). \tag{11}$$

In Eq. 10 we restrict the number of active centers to a constant. In Eq. 11 the number of electrons is held constant. Because of Eq. 11, the analysis which follows applies only to a system which has been given an average of $\bar{n}$ electrons per active center; i.e.

$$N_e = \bar{n} N_b.$$

We would like now to minimize F and find the equilibrium set $\{N_n\}$ for a particular $\bar{n}$. Using Eqs. 7–9 and Stirling's approximation (see for example ref. 15)

$$\ln N! = N \ln N - N, \tag{12}$$

we have

$$F = \sum_{n=0}^{8} N_n F_n - kT \left[N_b \ln N_b - \sum_{n=0}^{8} N_n \ln N_n \right]. \tag{13}$$

We minimize F subject to conditions 10 and 11 by using the Lagrange multiplier technique (15). The conditions for an extremum of F are (15)

$$(\partial F/\partial N_n) + a(\partial g_1/\partial N_n) + b(\partial g_2/\partial N_n) = 0, \quad n = 0, 1, \ldots, 8, \tag{14}$$

where a and b are Lagrange multipliers and g_1 and g_2 are given by Eqs. 10 and 11. From Eq. 13 we get

$$\partial F/\partial N_n = F_n + kT \ln N_n + kT. \tag{15}$$

Also

$$\partial g_1/\partial N_n = 1 \quad \text{and} \quad \partial g_2/\partial N_n = n - \bar{n}. \tag{16}$$

Putting Eqs. 15 and 16 into 14 we get

$$F_n + kT \ln N_n + kT + a + (n - \bar{n})b = 0. \tag{17}$$

Solving Eq. 17 for N_n gives

$$N_n = C e^{-[F_n + (n-\bar{n})b/kT]}, \tag{18}$$

where

$$C = e^{-(1 + a/kT)}. \tag{19}$$

For $n = 0, F_n = 0$ and thus,

$$N_0 = C e^{\bar{n}b/kT}. \tag{20}$$

Putting Eqs. 20 and 6 into 18 we get

$$N_n = N_0 Z_n e^{-nb/kT}. \tag{21}$$

Eqs. 11 and 21 can be used to evaluate b for a particular $\bar{n}$, i.e.

$$\sum_{n=0}^{8} (n - \bar{n}) Z_n e^{-nb/kT} = 0. \tag{22}$$

As can be seen, the value of b depends on $\bar{n}$. $b_{\bar{n}}$ is evidently something like a Fermi energy and increases as more electrons are added per active site.

In summary then, the following three equations are used to calculate the one-electron energies:

$$\sum_{n=0}^{8} (n - \bar{n}) Z_n e^{-nb_{\bar{n}}/kT} = 0 \tag{23}$$

$$N_{\bar{n}n} = N_{\bar{n}o} Z_n e^{-nb_{\bar{n}}/kT} \tag{24}$$

$$P_{\bar{n}j} = \sum_{n=0}^{8} (N_{\bar{n}n}/N_b) P_{nj}. \tag{25}$$

The $P_{\bar{n}j}$ are the probabilities for observing different species (e.g., j = Mo^{5+}, $FADH^{\cdot}$, $FADH_2$, ...) when there is an average of $\bar{n}$ electrons per active site. Z_n and P_{nj} are discussed in the text (Eqs. 1 and 2). Both depend on the relative one-electron energies. Thus one would vary these one-electron energies until a satisfactory fit is made to a $P_{\bar{n}j}$ vs. $\bar{n}$ figure (e.g. Fig. 3 of ref. 6) for all $\bar{n}$ and j. Eq. 23 is used to evaluate $b_{\bar{n}}$. This procedure is fairly complicated if used alone. We have used it only as a check on our values of E_j as derived in the text.

I would like to thank Professor Otto Theimer for his very helpful suggestions concerning the statistics involved in calculating the one-electron energies, especially those done in the Appendix.

Received for publication 29 May 1975 and in revised form 15 March 1976.

REFERENCES

1. MASSEY, V., P. E. BRUMBY, H. KOMAI, and G. PALMER. 1969. Studies on milk xanthine oxidase: some spectral and kinetic properties. *J. Biol. Chem.* **244**:1682.
2. PALMER, G., R. C. BRAY, and H. BEINERT. 1964. Direct studies on the electron transfer sequence in xanthine oxidase by electron paramagnetic resonance spectroscopy. I. Techniques and description of spectra. *J. Biol. Chem.* **239**:2657.
3. BRAY, R. C., G. PALMER, and H. BEINERT. 1964. Direct studies on the electron transfer sequence in xanthine oxidase by electron paramagnetic resonance spectroscopy. II. Kinetic studies employing rapid freezing. *J. Biol. Chem.* **239**:2667.
4. EDMUNDSON, D., D. BALLOU, A. VAN HEUVELEN, G. PALMER, and V. MASSEY. 1973. Kinetic studies on substrate reduction of xanthine oxidase. *J. Biol. Chem.* **248**:6135.
5. VAN HEUVELEN, A. 1975. Kinetic studies of electron transport reactions at low temperatures in xanthine oxidase. *Biochem. Biophys. Res. Commun.* **64**:963.
6. OLSON, J. S., D. P. BALLOU, G. PALMER, and V. MASSEY. 1974. The mechanism of action of xanthine oxidase. *J. Biol. Chem.* **249**:4363.

7. STEPHEN, H., and T. STEPHEN, eds. 1963. Solubilities of Inorganic and Organic Compounds, Volume I, Part 1. The MacMillan Company, New York. 575.
8. OLSON, J. S., D. P. BALLOU, G. PALMER, and V. MASSEY. 1974. The reaction of xanthine oxidase with molecular oxygen. *J. Biol. Chem.* **249**:4350.
9. LOWE, D. J., R. M. LYNDEN-BELL, and R. C. BRAY. 1972. Spin-spin interaction between molybdenum and one of the iron-sulphur systems of xanthine oxidase and its relevance to the enzymic mechanism. *Biochem. J.* **130**:230.
10. WILLIAMS, R. J. P. 1969. Electron Transfer and Energy Conservation. *Curr. Top. Bioenerg.* **3**:79.
11. GLASSTONE, S., K. J. LAIDLER, and H. EYRING. 1941. *In* The Theory of Rate Processes. McGraw Hill, Inc., New York. 197.
12. VAN HEUVELEN, A. 1973. Electron transfer mechanisms in electron transport chains. *J. Biol. Phys.* **1**:215.
13. LOWE, D. J., and J. S. HYDE. 1975. Electron-electron double resonance measurements on xanthine oxidase. *Biochem. Biophys. Acta.* **377**:205.
14. BENNETT, L. E. 1973. Metalloprotein redox reactions. *Prog. Inorg. Chem.* **18**:1.
15. TER HAAR, D. 1960. Elements of Statistical Mechanics. Holt, Rinehart and Winston, New York. 444.